# Tandem-L: mission performance and optimization for repeat-pass interferometry.

Francesco De Zan, Michael Eineder, Gerhard Krieger, Alessandro Parizzi, Pau Prats
DLR (German Aerospace Center), P.O. Box 1116, 82230 Wessling, Germany
francesco.dezan@dlr.de, tel. +49 (0) 8153 28 2150, fax +49 (0) 8153 28 1135

## Abstract

The Tandem-L mission proposal has a high potential for deformation-monitoring applications. With a short revisit time at L-band, high coherence is expected over a variety of artificial and natural structures. Its wide swath will enable geological applications that are concerned with small motions over large distances. We present performance studies showing trades in the mission design, like revisit time and look number. We use performance models from the literature, integrated with temporal coherence and atmosphere characterizations from studies with available sensors. We discuss the impact of adding some left-looking acquisitions to the normal right-looking acquisition plan.

## 1 Overview

With the Tandem-L study we are facing the problem of designing and optimizing an L-band satellite SAR mission for repeat-pass differential interferometry (see [2]). In reality we face a more complex problem, since Tandem-L is intended to serve further applications (see [1]), but this will not be discussed here. With the aim of carrying out performance and trade-off studies we have adopted performance models for multi-pass interferometry. Such models are general enough so that they can describe a variety of situations (decorrelation and atmospheric disturbance characterization, deformation models). However, we are aware of the presence of needs that have not been formalized in the performance models.
In the context of mission planning we want to consider trades between different system and observation parameters so that we can give answers to questions like "Do we prefer high resolution or frequent revisits?" or "Will we gain from alternating left and right looking acquisitions for 2-D deformation retrieval?"
It will be clear that for some question there is no easy answer and an important role is played by our assumptions on propagation and phase disturbances and on the scatterers' temporal stability.

## 2 Two- or three-D performance for long series

With a short revisit time and a systematic acquisition plan Tandem-L will acquire long series of wide-swath images. Geological applications are particularly interested in this kind of data, as they have the potential of recovering weak deformation signals over large distances.
We assume for the processing of these images that we are interested in some slow and continuous motion that can be modeled by a constant velocity. Such a motion would be low-pass in space so that it will make sense to average the interferometric phases over a certain number of looks. The averaging window will be small enough so that propagation phase disturbances can be considered constant within the window.
We follow for the performance of stacks (see also [3]) the most likely processing steps. First we estimate the accuracy in each line of sight (LoS), then combine the different LoS to derive the performance of the 2-3D motion reconstruction. A Cramér-Rao lower bound found in the literature ([4] and [5]) gives the performance for each LoS, as a function of the sampling times, the number of looks, the coherence matrix (characterizing how each image is able to interfere with each other) and the atmospheric noise power. The combination of the various directions to get a 2- or 3-dimensional velocity vector follows the analysis in [8] and [9], which is just an optimal linear combination of the various 1-D measures.

### 2.1 Modeling of coherence and phase disturbances

The interferometric performance depends strongly on the coherence matrix ($\Gamma$) of our data and the phase disturbance characterization. Concerning coherence we adopt the following simple model, where the coherence is essentially a function of the time separation $|t_n - t_k|$ of the image pair (geometric decorrelation is expected to be practically irrelevant, due to the bandwidth and tight orbit control). For $n \neq k$:

$$\Gamma(n,k) = (\gamma_0 - \gamma_\infty)\exp(-|t_n - t_k|/\tau) + \gamma_\infty \quad (1)$$

where $\gamma_0$ is the coherence at short time lags (a few days), $\gamma_\infty$ is the level for long time lags (in our case, something like 5 years), $\tau$ describes the transition velocity. This model has been applied to an ALOS/PALSAR dataset and an example is given in **Figure 1**. In the following we will assume that $\gamma_0 = 0.8$, $\gamma_\infty = 0.2$ and $\tau = 60$ days.
Similar results for the L-band coherence behavior can be found in another study (see [11]), where one can also ob-

serve coherence long-term leveling off in the range 0.2 - 0.4. A hint on the validity of the same model at shorter time scales is given in the observations made in [12] over forest. Of course a more comprehensive modeling should distinguish between different terrain types and climates. For instance ice can have a much faster coherence decay.

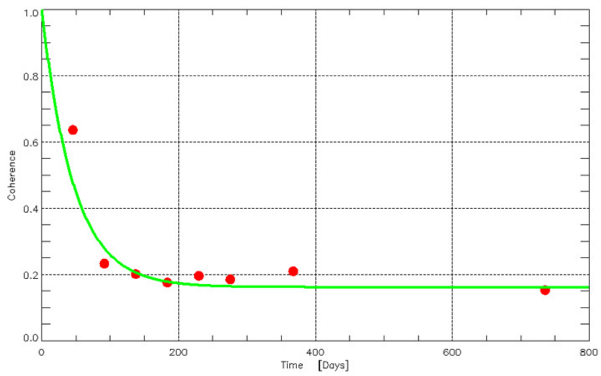


**Figure 1:** Example of L-band decorrelation as a function of time. The dots represent coherences in a ALOS/PALSAR dataset over a Greek island.

Concerning tropospheric propagation disturbances, we have surveyed different studies and found that a typical reported zenith differential delay is 1cm at a distance of 50 km. After converting this number to the corresponding phase and accounting for the incidence angle we have that each image would be affected by about 0.5 rad at L-band (standard deviation). We use this number in the following analysis, being aware that also here a dependence on local climate would be needed for a better description. We decide to ignore phase errors that could result from errors in the DEM used to compensate the topographic phase because of the capability of Tandem-L to generate its own L-band DEM with a single-pass interferometer and the tight orbital control which is currently foreseen.

## 2.2 First analysis

Using the above-mentioned assumptions about coherence, atmospheric disturbance and linear motion estimation, **Figure 2** reports the predicted performance as a function of the number of images. The various contributions are isolated to be better understood. What is immediately clear is that system additive noise contributions are not critical, thanks to multilooking. The effect of system noise on coherence is the same as the sudden loss of temporal coherence that we will anyway experience with acquisitions a few days apart. The decorrelation of the target will easily mask system noise, for example, when it is lower than 10 dB, since a starting coherence $\gamma_0 = 0.8$ corresponds to an SNR of about 7 dB. Even with a higher starting coherence the effect of system noise will be minor after a few acquisitions.

The effect of atmosphere is mitigated as the number of images is increased. The followed approach doesn't consider the possibility of using point targets (Persistent Scatterers) that stay coherent over the whole mission time. These targets can have even better performances against phase disturbances but their presence and density over natural terrains would require further analyses. In any case the information from interferogram multilooking and isolated high-quality targets should be integrated in a processing or post processing step.

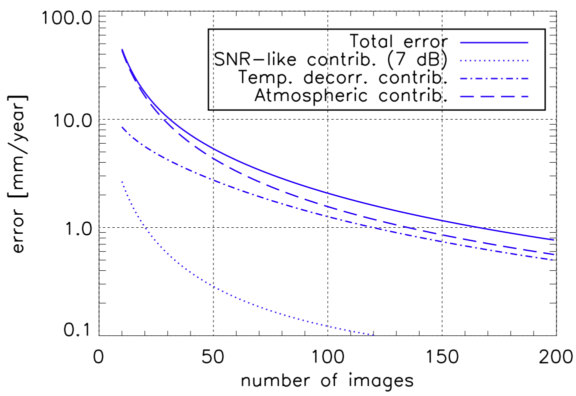


**Figure 2:** Components of the predicted estimation error as a function of number of images (with 8-day repeat cycle), for 100 looks.

## 2.3 Resolution vs. revisit trade

One interesting trade is between the resolution and the revisit interval. Of course we would like to have both a high resolution and frequent acquisitions but what if we are given a maximum data rate to be acquired and we have to stick to a regular schedule? In **Figure 3** we show the performance for different observation frequencies, where the resolution is adapted to keep the data volume constant (i.e. more frequent acquisitions imply lower number of looks). The plots are given under different atmospheric noise conditions, from half to the double of what was assumed so far. For high atmospheric noise values, frequent revisits are strongly preferred (atmosphere stacking). For low values the optimum migrates towards longer revisits, but the quality becomes much more uniform. As far this analysis can tell, the choice of the 8-day repeat is a good one.
The frequent revisit has further advantages (and possibly disadvantages) which are not fully captured by our performance model. For sure a frequent revisit allows for a better phase sampling, making spatial multilooking easier. This will be especially true for fast and erratic motions, where an *a priori* deformation model will not be possible. The biggest benefit will be for ice applications because of need to detect fast movements.

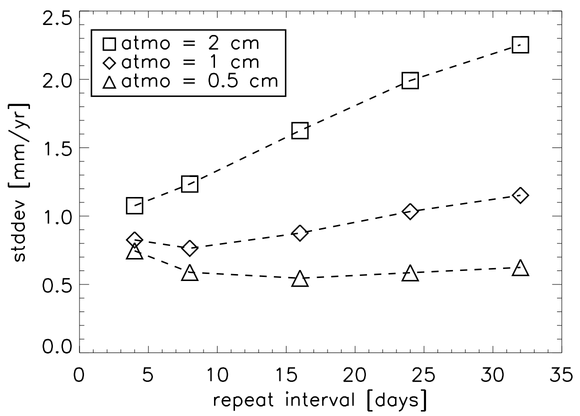


**Figure 3:** Resolution / repeat-pass trade (100 looks @ 8 days) for different atmospheric delay standard deviations. The product of repeat-pass interval and 2-D resolution is assumed constant (i.e. constant data volume).

## 2.4 Subsampling and additional LoS

Due to conflicts with other acquisitions the wide-swath series dedicated to solid Earth applications might be interrupted from time to time or regularly. We want to assess the impact of missing acquisitions. Another reason could be to operate the radar in a left-looking mode for a couple of repeat cycles every six so to acquire an additional line of sight. In this case according to the models, the loss in the right-looking geometry is very small as one can see in **Figure 4**.

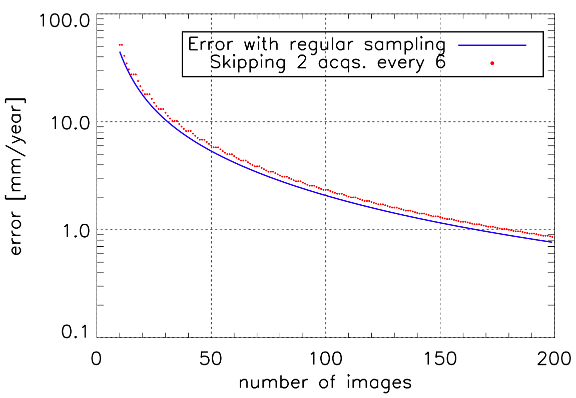


**Figure 4:** The effect of skipping two consecutive acquisitions every six. At the end of the mission the accuracy worsens from 0.76 to 0.86 mm/year, i.e. we lose about 1dB.

The gain in the 2-D motion reconstruction (North-South component is ignored) is shown in **Figure 5** and **6**. It has been obtained with simulations of a 5 year mission with regular switching between right and left looking. For each viewing geometry we consider acquisitions from both ascending and descending passes.

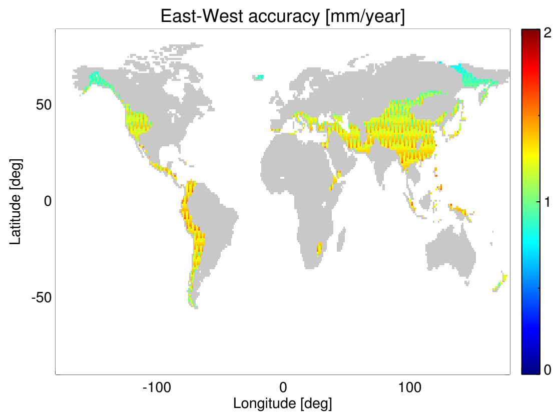


**Figure 5:** East-West accuracy when using only right-looking acquisitions.

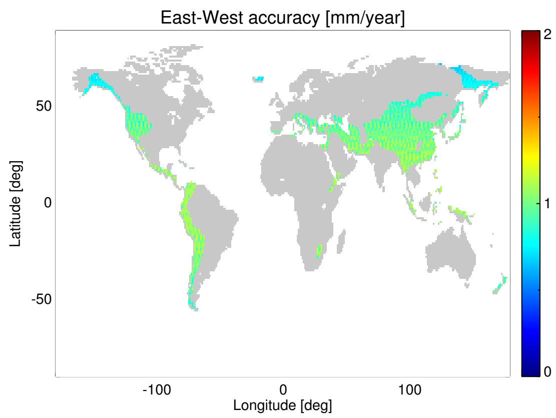


**Figure 6:** East-West accuracy substituting 2 consecutive right-looking acquisitions every 6 (i.e. one third) with left-looking.

It turn out that the performance loss from the reduced number of viewing directions is mor then compensated by the additional left-looking acquisitions.

# 3 Conclusions

In this paper we have investigated some trades in the context of long time deformation monitoring with Tandem-L. This has been possible using performance models and additional information, like the characterization of temporal coherence properties in L-band and of atmospheric delay at the spatial scale of interest. We have studied the impact of the revisit time under the constraint of constant data volume and we have shown the benefit of introducing some left-looking acquisitions, even at the expenses of right-looking.

# References


[1] G. Krieger et al. "The Tandem-L Mission Proposal: Monitoring Earth's Dynamics with High Resolution SAR Interferometry," *Proceedings of IEEE Radar Conference*, 2009

[2] M. Eineder et al., "Scientific Requirements and Feasibility on an L-band Mission dedicated to Measure Surface Deformation," *Proceedings of IGARSS 2009*, pp.1–4, [to be published]

[3] F. De Zan et al., "Mission design and performance for systematic deformation measurements with a spaceborne SAR system," *Proceedings of IGARSS 2009*, pp.1–4, [to be published]

[4] A. Monti Guarnieri and S. Tebaldini, "Hybrid Cramér-Rao bound for crustal displacement field estimators in SAR interferometry," *IEEE Signal Proc. Letters*, vol. 14, pp. 1012–1015, December 2007.

[5] A. Monti Guarnieri and S. Tebaldini, "On the exploitation of target statistics for SAR interferometry applications," *IEEE Trans. Geosci. Remote Sensing*, vol. 46, pp. 3436–3443, November 2008.

[6] T.R. Emardson et al., "Neutral atmospheric delay in interferometric synthetic aperture radar applications: statistical description and mitigation," *J. Geophys. Res.*, vol. 108, pp. ETG 4.1–ETG 4.8, May 2003.

[7] R.F. Hanssen, *Radar Interferometry*, Kluwer Academic Press, 2001.

[8] T. J. Wright et al., "Toward mapping surface deformation in three dimensions using InSAR," *Geophysical Research Letters*, vol. 31, pp. L01607.1–L01607.5, January 2004.

[9] F. Rocca, "3D motion recovery with multi-angle and/or left right interferometry," *Proc. of Fringe 2003 Workshop*, pp. 1–5, June 2004.

[10] A Parizzi et al. "First Results from Multifrequency Interferometry - A comparison of different Decorrelation Time Constants at X, C and L-band," at Fringe 2009 Workshop

[11] M. Shimada et. al, "The polarimetric and interferometric potential of ALOS PALSAR" *Proc. of POLinSAR 2005 Workshop*, pp. 1–6, May 2005.

[12] S.-K. Lee et al., "The Impact of Temporal Decorrelation over Forest Terrain in Polarimetric SAR Interferometry" *Proc. of POLinSAR 2009 Workshop*, pp. 1–6, April 2009.